



This discussion paper is/has been under review for the journal Atmospheric Chemistry and Physics (ACP). Please refer to the corresponding final paper in ACP if available.

# Implications of model bias in carbon monoxide for methane lifetime

S. A. Strode<sup>1,2</sup>, B. N. Duncan<sup>2</sup>, E. A. Yegorova<sup>2,3,a</sup>, J. Kouatchou<sup>2,4</sup>,  
J. R. Ziemke<sup>2,5</sup>, and A. R. Douglass<sup>2</sup>

<sup>1</sup>Universities Space Research Association, Columbia, MD, USA

<sup>2</sup>NASA Goddard Space Flight Center, Greenbelt, MD, USA

<sup>3</sup>Earth System Science Interdisciplinary Center, College Park, MD, USA

<sup>4</sup>Science Systems and Applications Inc., Lanham, MD, USA

<sup>5</sup>Morgan State University, Baltimore, MD, USA

<sup>a</sup>now at: Nuclear Regulatory Commission, Rockville, MD, USA

Received: 1 June 2015 – Accepted: 1 July 2015 – Published: 27 July 2015

Correspondence to: S. Strode (sarah.a.strode@nasa.gov)

Published by Copernicus Publications on behalf of the European Geosciences Union.

## Implications of model bias in carbon monoxide for methane lifetime

S. A. Strode et al.

Title Page

Abstract

Introduction

Conclusions

References

Tables

Figures



Back

Close

Full Screen / Esc

Printer-friendly Version

Interactive Discussion



## Abstract

A low bias in carbon monoxide (CO) at high northern latitudes is a common feature of chemistry climate models (CCMs) that may indicate or contribute to a high bias in simulated OH and corresponding low bias in methane lifetime. We use simulations with CO tagged by source type to investigate the sensitivity of the CO bias to CO emissions, global mean OH, and the hemispheric asymmetry of OH. Our results show that reducing the hemispheric asymmetry of OH improves the agreement of simulated CO with observations. We use simulations with parameterized OH to quantify the impact of known model biases on simulated OH. Removing biases in ozone and water vapor as well as reducing Northern Hemisphere NO<sub>x</sub> does not remove the hemispheric asymmetry in OH, but brings the simulated methyl chloroform lifetime into agreement with observation-based estimates.

## 1 Introduction

Carbon monoxide (CO) is an ozone precursor and the primary sink of the hydroxyl radical (OH) in the troposphere. Consequently, CO indirectly impacts climate by increasing tropospheric ozone and increasing the lifetimes of methane and other short lived greenhouse gases (GHGs), as well as eventually oxidizing to CO<sub>2</sub> (e.g. Prather, 1996; IPCC, 1990). The effect of CO on OH also leads to impacts on oxidation of SO<sub>2</sub> to sulfate, providing another climate forcing (Shindell et al., 2009). Previous studies calculated global warming potentials due to these effects using box models (Daniel and Solomon, 1998), 2-dimensional models (Fuglestedt et al., 1996; Johnson and Derwent, 1996), or 3-dimensional models (Derwent et al., 2001; Fry et al., 2013, 2012; Berntsen et al., 2005; Shindell et al., 2009). Since neither CO nor ozone is well mixed in the atmosphere, the location of the CO perturbation affects its climate impact. CO emissions in the tropics have a greater impact on ozone radiative forcing than emissions at high latitudes (Bowman and Henze, 2012) due the intense photochemistry in the tropics as

## Implications of model bias in carbon monoxide for methane lifetime

S. A. Strode et al.

Title Page

Abstract

Introduction

Conclusions

References

Tables

Figures



Back

Close

Full Screen / Esc

Printer-friendly Version

Interactive Discussion







**Implications of model bias in carbon monoxide for methane lifetime**

S. A. Strode et al.

[Title Page](#)[Abstract](#)[Introduction](#)[Conclusions](#)[References](#)[Tables](#)[Figures](#)[◀](#)[▶](#)[◀](#)[▶](#)[Back](#)[Close](#)[Full Screen / Esc](#)[Printer-friendly Version](#)[Interactive Discussion](#)

is to quantify the relationship of the extratropical NH CO bias seen in chemistry climate models with bias in oxidant concentrations and methane lifetime. We use the GEOS-5 Chemistry Climate Model (GEOSCCM) to compare the impact of increasing CO emissions vs. reducing OH concentrations on the CO distribution. We also quantify the contribution of model biases in other constituents such as ozone and water vapor to the simulated OH and CO distributions and methane lifetime.

## 2 Methods

### 2.1 Constituent observations and assimilated fields

Our primary constraint on the model CO distribution comes from surface observations of CO from the NOAA Global Modeling Division (GMD) network (Novelli and Masarie, 2014). We use the monthly mean data. The MOPITT instrument on the TERRA satellite provides additional constraints on the CO distribution. MOPITT provides almost global coverage of CO every three days from March 2000 to present (Edwards et al., 2004). We use the level 3 CO column data from the MOPITT version 5 thermal infrared (TIR) product (Deeter et al., 2011, 2013).

Observations of tropospheric ozone are important for constraining the source of OH. Ziemke et al. (2011) created a climatology of tropospheric column ozone (TCO) based on the difference between the stratospheric column ozone (SCO) from the Microwave Limb Sounder (MLS) and total ozone column data from the Ozone Monitoring Instrument (OMI). We use the TCO product for 2004–2010 to constrain the tropospheric ozone column. Stratospheric ozone is also important for constraining the OH source due to its effect on photolysis (Rohrer and Berresheim, 2006). We use the Global Modeling and Assimilation Office (GMAO) ozone assimilation product for 2005–2010 to constrain stratospheric ozone concentrations. The GMAO assimilated ozone product, described in Ziemke et al. (2014) and Wargan et al. (2015), is a gridded product that

ingests MLS ozone profiles and OMI total column ozone into the GEOS-5 assimilation system.

Water vapor is another important influence on OH concentrations. We use specific humidity from the Modern-Era Retrospective Analysis for Research and Applications (MERRA) (Rienecker et al., 2011).

## 2.2 Model and methodology

Our analysis uses several chemistry options within the GEOSCCM framework to assess possible causes and impacts of CO and OH bias. After spin-up, we conduct a series of time slice simulations of 1999–2009 with fixed emissions using observed sea surface temperatures (SSTs) to drive the CCM meteorology, and then average our results over all years of the time slice. All simulations use the Fortuna version of GEOS-5 (Molod et al., 2012) and have 2° latitude by 2.5° longitude horizontal resolution and 72 vertical levels. We describe each chemistry option and associated experiments below and in Table 1.

### 2.2.1 GMI chemistry option

GEOSCCM integrates the chemistry mechanism of the Global Modeling Initiative (GMI) CTM (Duncan et al., 2007b; Strahan et al., 2007) into the GEOS-5 AGCM. The GMI chemistry includes a comprehensive mechanism of tropospheric and stratospheric chemistry, including 117 species and over 400 reactions. The reference simulation for this study, hereafter called RefGMI, is the year 2000 timeslice simulation conducted for the ACCMIP intercomparison. The configuration of the ACCMIP simulations is described in Lamarque et al. (2013). The biases in CO and methane lifetime seen in the GEOSCCM simulation are similar to those seen in the ACCMIP multi-model mean (Naik et al., 2013). Consequently, our analyses of bias in the GEOSCCM are likely applicable to other chemistry climate models as well.

## Implications of model bias in carbon monoxide for methane lifetime

S. A. Strode et al.

Title Page

Abstract

Introduction

Conclusions

References

Tables

Figures



Back

Close

Full Screen / Esc

Printer-friendly Version

Interactive Discussion



## Implications of model bias in carbon monoxide for methane lifetime

S. A. Strode et al.

Title Page

Abstract

Introduction

Conclusions

References

Tables

Figures



Back

Close

Full Screen / Esc

Printer-friendly Version

Interactive Discussion



We conduct a sensitivity simulation, described in Sect. 3.2, that is identical to the ACCMIP simulation except for an increase in CO emissions. We refer to this simulation as GMI-HiEmis. Since trace gases in the GMI option of the GEOSCCM are radiatively coupled to the underlying GCM, altering emissions within this option produces feed-backs between CO, O<sub>3</sub>, CH<sub>4</sub>, and radiation and transport.

### 2.2.2 CO-only option

GEOSCCM includes a CO-only option to “tag” CO according to source type or location (Bian et al., 2010). This simplified chemistry option allows us to separate the contributions of different CO sources and to quantify the impact of a specific change in OH. In this chemistry option, the loss of CO is calculated based on prescribed OH fields, so changes in CO do not feed back onto OH. Our reference tagged-CO simulation, called RefCOonly, uses monthly OH fields archived from the GEOSCCM ACCMIP simulation, and the CO sources from methane and isoprene oxidation are calculated using monthly methane and isoprene fields archived from the ACCMIP simulation as well. Emissions and other forcings are chosen to parallel the ACCMIP simulation; however, the COonly option includes an amplification factor for CO emissions to account for the absence of co-emitted NMHCs (Duncan et al., 2007a). Section 3.2 describes CO-only sensitivity studies.

The GEOSCCM includes an option to constrain the meteorology with MERRA or any GMAO assimilation product. The simulation is pulled towards the MERRA analysis through application of an incremental analysis update (Bloom et al., 1996), calculated every six hours from comparison of the simulation with the analysis. We conduct a COonly simulation with specified dynamics from MERRA, which we refer to as COonlySD. The COonlySD simulation has the same emissions and OH field as RefCOonly, but the tracer transport will differ between the two simulations.



5 tropospheric OH of  $11.2 \pm 1.3$  years. The lifetimes of methyl chloroform and methane against tropospheric OH in the RefGMI simulation are 5.9 and 9.6 years, respectively (Table 2). The lifetimes of methyl chloroform and methane against tropospheric OH in the RefCO-OH simulation are 6.4 and 10 years, respectively, within the uncertainty of the observation-based estimates. The seasonal cycles are similar in both simulations, but the difference in NH OH is larger in the first half of the year than the second half (Fig. 1d). Consequently, when using the CO-OH parameterization to investigate OH and CO, we present the changes due to a given factor rather than the absolute values of CO, OH, and methane lifetime for easier comparison with the other simulations.

### 10 3 Results

We use the three chemistry options of the GEOSCCM to separate the contributions of emissions, chemistry, and transport to model bias in CO and methane lifetime. Section 3.1 compares the CO distribution simulated by the three options to observations and discusses the consistencies and differences between simulations. We analyze the impacts of increasing emissions, decreasing OH, and changing model transport on the CO distribution in Sect. 3.2, and examine how changing CO emissions affects ozone and OH in Sect. 3.3. Section 3.4 investigates the contribution of known model biases to the simulated OH and methane lifetime. Table 1 summarizes the key results of each of the sensitivity studies.

#### 20 3.1 Comparison of CO in the reference simulations and observations

This section presents a comparison of CO and OH distributions from the RefGMI, RefCO-only, and RefCO-OH simulations to each other and to observations. Figure 2 compares the annual cycle of CO in simulations to observations from six GMD sites selected to represent a range of latitudes. The RefGMI simulation (purple) is biased low at the NH sites, with the bias most prominent in the first half of the year, especially

## Implications of model bias in carbon monoxide for methane lifetime

S. A. Strode et al.

Title Page

Abstract

Introduction

Conclusions

References

Tables

Figures



Back

Close

Full Screen / Esc

Printer-friendly Version

Interactive Discussion



## Implications of model bias in carbon monoxide for methane lifetime

S. A. Strode et al.

Title Page

Abstract

Introduction

Conclusions

References

Tables

Figures

◀

▶

◀

▶

Back

Close

Full Screen / Esc

Printer-friendly Version

Interactive Discussion



NH spring. The simulation shows less bias at the SH sites, but some negative bias is evident in SH spring. The RefCOonly simulation (green) shows similar results to RefGMI, including a large negative bias in the NH in spring. Consequently, diagnosing the cause of bias in the RefCOonly simulation can provide insight into the bias in the RefGMI simulation.

The RefCO-OH simulation (orange) shows less springtime bias compared to observations than the RefGMI and RefCOonly simulations. However, its annual cycle is shifted later, resulting in more negative biases in September–December at the higher northern latitudes. The difference between the RefCO-OH and the other two reference simulations is explained by the differences in the OH field calculated by the parameterization compared to that calculated by the GMI chemistry mechanism. In April, when the greater NH bias of the RefGMI simulation is most evident (Fig. 2), the RefGMI OH is markedly higher than the RefCO-OH OH (Fig. 1).

### 3.2 Sensitivity of simulated CO to sources, OH, and transport

#### 3.2.1 Sensitivity of CO-only simulations to sources and OH

Adjusting the strength of mid-latitude CO sources can reduce the bias in the interhemispheric CO gradient. We use CO-only simulations to examine the impact of increasing specific sources of CO. Following the method of Strode and Pawson (2013), we estimate the impact of increasing a particular source by increasing the tagged-CO tracer for that source and then re-computing total CO. We impose increases of 10, 20, 50, 100, and 150% for each tagged tracer. Figure 3 shows how the increased Asian anthropogenic CO (CO<sub>aa</sub>) or tropical biomass burning CO (CO<sub>trbb</sub>) alters the comparison between modeled CO and the GMD CO observations as a function of latitude taken as an average of March to August. Similar results are present for spring and summer individually. An increase in CO<sub>aa</sub> of approximately 100% removes the negative bias at high latitude sites, but has little effect on the small negative bias at low latitudes (Fig. 3a). CO transported southward from Asia encounters higher OH than that trans-

ported northward, leading to a shorter lifetime (Duncan and Logan, 2008). Increasing CO<sub>trbb</sub> improves the model agreement with observations at low latitudes, but creates overestimates at some tropical sites while providing only a modest reduction in the high latitude bias (Fig. 3b).

We examine the impact of reducing OH concentrations globally or only in the NH in our CO<sub>only</sub> simulation and find that a large decrease in NH OH is effective in reducing the high latitude CO bias. Naik et al. (2013) found that the ACCMIP multi-model mean underestimated tropospheric OH by 5–10% globally. The NH/SH OH ratios in the ACCMIP multi-model mean and GEOSCCM ACCMIP simulation are 1.28 and 1.18, respectively (Naik et al., 2013), compared to the (Patra et al., 2014) estimate of  $0.97 \pm 0.12$ . Figure 3c shows that reducing OH by 5–10% leads to a small increase in CO across all latitudes, yielding a small reduction in the bias compared to GMD observations. Decreasing OH by 20% in the NH only leads to a large improvement in high latitude CO compared to observations, with only a small effect in the Southern Hemisphere.

### 3.2.2 Impact of sources and OH on global mean and IHG bias in CO

We find that achieving zero bias in both the IHG and the global mean would require changes in multiple emission sources. Figure 4 illustrates how changing the concentrations of several tagged CO tracers, as well as OH, impacts the global mean bias, inter-hemispheric gradient (IHG) bias, and correlation ( $r^2$ ) of the simulated CO compared to the GMD observations for March through May. Increasing anthropogenic CO from Asia (CO<sub>aa</sub>), Europe (CO<sub>ea</sub>), or North America (CO<sub>na</sub>), or increasing Russian biomass burning (CO<sub>rub</sub>) reduces the bias in the IHG as well as the global mean. Increasing CO from tropical biomass burning (CO<sub>trbb</sub>) leads to a smaller reduction in the IHG bias, while increasing CO from biogenic emissions (CO<sub>bio</sub>) reduces the mean bias with little effect on the IHG (Fig. 4a). Consequently, increases in both groups of emissions are necessary to simultaneously remove the global mean bias and correct the IHG.

## Implications of model bias in carbon monoxide for methane lifetime

S. A. Strode et al.

Title Page

Abstract

Introduction

Conclusions

References

Tables

Figures



Back

Close

Full Screen / Esc

Printer-friendly Version

Interactive Discussion











the tropospheric ozone photolysis rate, specific humidity, and reactive nitrogen emissions, and inversely proportional to CO emissions. Here, we examine the sensitivity of OH to model biases in some of these factors.

### 3.4.1 Sensitivity to tropospheric ozone

5 Comparison of the CCMs that participated in the ACCMIP study to OMI/MLS TCO reveals positive biases in simulated tropospheric ozone over the NH midlatitudes, and negative biases over the tropical Pacific and SH (Young et al., 2013), which leads to an overestimate in NH OH production and an underestimate in SH OH production (Naik et al., 2013). The multi-model mean tropospheric ozone also shows a high bias in the  
10 NH and low bias in the SH compared to the Tropospheric Emission Spectrometer (TES) (Bowman et al., 2013). A multi-species assimilation study by Miyazaki et al. (2012) found that assimilating TES ozone increased OH concentrations in the SH.

We use the CO-OH parameterization to investigate the impact of removing the GEOSCCM's tropospheric ozone column bias relative to the OMI/MLS observations  
15 (Fig. 9). We scale the tropospheric ozone values input to the parameterization for each month between October 2004 and December 2010 from 60° S–60° N so that the tropospheric ozone column is unbiased compared to the OMI/MLS TCO for that month. We use the scaled ozone input in a sensitivity study for October 2004 to January 2010, called CO-OHSensTCO, which parallels the RefCO-OH simulation but uses  
20 the scaled tropospheric ozone values in the OH parameterization. CO-OHSensTCO shows a small (2 %) decrease in global mean OH compared to RefCO-OH, with a 3 % decrease in NH OH and 1 % decrease in SH OH. The increased OH leads to a 2 % increase in both methane and methyl chloroform lifetimes against OH. The NH/SH OH ratio decreases slightly to 1.19 (Table 4), suggesting that the inter-hemispheric gra-  
25 dent in the tropospheric ozone bias makes only a minor contribution to the model's interhemispheric OH asymmetry.

## Implications of model bias in carbon monoxide for methane lifetime

S. A. Strode et al.

Title Page

Abstract

Introduction

Conclusions

References

Tables

Figures



Back

Close

Full Screen / Esc

Printer-friendly Version

Interactive Discussion



### 3.4.2 Sensitivity to stratospheric ozone

We next examine how biases in stratospheric ozone affect OH through their role in photolysis. Voulgarakis et al. (2013) found that changes in stratospheric ozone and tropospheric OH in the ACCMIP models both correlated strongly with  $J(O^1D)$ . We conduct a sensitivity study for 2005 through 2009, CO-OHSensStO3, which parallels the RefCO-OH simulation but replaces the simulated ozone with the GMAO ozone assimilation in the stratosphere for input into the parameterization. The change in global mean OH in CO-OHSensStO3 is nearly identical to that of CO-OHSensTCO, but CO-OHSensStO3 places more of the change in the SH, causing the NH/SH OH ratio to increase to 1.23 (Table 4). The change in OH due to stratospheric ozone bias is small in part because GEOSCCM has relatively small biases in tropical stratospheric ozone. However, the multi-model Chemistry Climate Model Validation-2 (CCMVal-2) study (Morgenstern et al., 2010) shows a large spread across models for column ozone in the tropics (Austin et al., 2010). Thus, biases in stratospheric ozone may play a larger role in tropospheric OH in models with larger stratospheric ozone biases.

### 3.4.3 Sensitivity to water vapor

We investigate the impact of model biases in water vapor on OH concentrations through its role in OH production. Inter-model differences in OH in the POLMIP study are correlated with inter-model differences in simulated water vapor (Monks et al., 2015). The GEOS-5 AGCM exhibits a high bias in specific humidity compared to the MERRA reanalysis in much of the troposphere (Molod et al., 2012), and a high bias in the mid-troposphere is also seen throughout the year in GEOSCCM compared to AIRS data (Lamarque et al., 2013).

We quantify the impact of this bias by conducting a sensitivity study, CO-OHSensQ, that applies altitude and latitude-dependent zonal mean scaling factors for each month to the specific humidity provided to the OH parameterization. The scaling factors are based on comparison of the RefGMI simulation to MERRA and are applied in 100 hPa

## Implications of model bias in carbon monoxide for methane lifetime

S. A. Strode et al.

Title Page

Abstract

Introduction

Conclusions

References

Tables

Figures



Back

Close

Full Screen / Esc

Printer-friendly Version

Interactive Discussion



## Implications of model bias in carbon monoxide for methane lifetime

S. A. Strode et al.

Title Page

Abstract

Introduction

Conclusions

References

Tables

Figures

⏪

⏩

◀

▶

Back

Close

Full Screen / Esc

Printer-friendly Version

Interactive Discussion



intervals between 900 and 200 hPa for 60° S to 60° N. These scaling factors are designed to remove the mean bias in the simulated specific humidity compared to MERRA while allowing the simulated water vapor to vary in space and time in a manner consistent with the simulated meteorology. The water vapor scaling is applied only to the OH parameterization, and does not impact the general circulation of the simulation. The scaling results in lower specific humidity in the middle and upper troposphere, with the largest percent reductions occurring between 300 and 500 hPa (Fig. 10).

Simulated OH is 6 % lower in the CO-OHSensQ simulation than the RefCO-OH simulation, and the methane and methyl chloroform lifetimes against OH are thus 6 % longer (Table 4). Consequently, water vapor bias has a larger impact on OH concentrations than the stratospheric or tropospheric ozone biases in our simulations. The OH reduction is similar in both hemispheres in the annual mean, so the NH/SH OH gradient is unchanged compare to RefCO-OH.

### 3.4.4 Sensitivity to NO<sub>x</sub>

Anthropogenic NO<sub>x</sub> emissions, which contribute to secondary production of OH, are located primarily in the Northern Hemisphere. Consequently, an overestimate of these emissions could contribute to the NH/SH asymmetry in simulated OH. We quantify the sensitivity of simulated OH to NH NO<sub>x</sub> with a sensitivity study, CO-OHSensNO<sub>x</sub>, which parallels RefCO-OH but includes 30 % lower NO<sub>x</sub> concentrations in the NH. This reduction in NH NO<sub>x</sub> emissions leads to a 3 % reduction in global OH (Table 4). SH and NH OH are reduced by 0.3 and 6 %, respectively, reducing the NH/SH OH ratio to 1.15. While this shows that the hemispheric asymmetry in OH is affected by NO<sub>x</sub> emissions, a much larger redistribution of NO<sub>x</sub> emissions would be required to completely eliminate the asymmetry.







## Implications of model bias in carbon monoxide for methane lifetime

S. A. Strode et al.

Title Page

Abstract

Introduction

Conclusions

References

Tables

Figures



Back

Close

Full Screen / Esc

Printer-friendly Version

Interactive Discussion

Frith, S., Garcia, R. R., Garny, H., Gettelman, A., Hardiman, S. C., Kinnison, D., Lamarque, J. F., Mancini, E., Marchand, M., Michou, M., Morgenstern, O., Nakamura, T., Pawson, S., Pitari, G., Pyle, J., Rozanov, E., Shepherd, T. G., Shibata, K., Teysedre, H., Wilson, R. J., and Yamashita, Y.: Decline and recovery of total column ozone using a multimodel time series analysis, *J. Geophys. Res.-Atmos.*, 115, D00M10, doi:10.1029/2010jd013857, 2010.

Berntsen, T. K., Fuglestvedt, J. S., Joshi, M. M., Shine, K. P., Stuber, N., Ponater, M., Sausen, R., Hauglustaine, D. A., and Li, L.: Response of climate to regional emissions of ozone precursors: sensitivities and warming potentials, *Tellus B*, 57, 283–304, doi:10.1111/j.1600-0889.2005.00152.x, 2005.

Bian, H. S., Chin, M. A., Kawa, S. R., Yu, H. B., Diehl, T., and Kucsera, T.: Multiscale carbon monoxide and aerosol correlations from satellite measurements and the GOCART model: implication for emissions and atmospheric evolution, *J. Geophys. Res.-Atmos.*, 115, D07302, doi:10.1029/2009jd012781, 2010.

Bloom, S. C., Takacs, L. L., da Silva, A. M., and Ledvina, D.: Data assimilation using incremental analysis updates, *Mon. Weather Rev.*, 124, 1256–1271, doi:10.1175/1520-0493(1996)124<1256:DAUIAU>2.0.CO;2, 1996.

Bowman, K. and Henze, D. K.: Attribution of direct ozone radiative forcing to spatially resolved emissions, *Geophys. Res. Lett.*, 39, L22704, doi:10.1029/2012gl053274, 2012.

Bowman, K. W., Shindell, D. T., Worden, H. M., Lamarque, J.F., Young, P. J., Stevenson, D. S., Qu, Z., de la Torre, M., Bergmann, D., Cameron-Smith, P. J., Collins, W. J., Doherty, R., Dalsøren, S. B., Faluvegi, G., Folberth, G., Horowitz, L. W., Josse, B. M., Lee, Y. H., MacKenzie, I. A., Myhre, G., Nagashima, T., Naik, V., Plummer, D. A., Rumbold, S. T., Skeie, R. B., Strode, S. A., Sudo, K., Szopa, S., Voulgarakis, A., Zeng, G., Kulawik, S. S., Aghedo, A. M., and Worden, J. R.: Evaluation of ACCMIP outgoing longwave radiation from tropospheric ozone using TES satellite observations, *Atmos. Chem. Phys.*, 13, 4057–4072, doi:10.5194/acp-13-4057-2013, 2013.

Daniel, J. S. and Solomon, S.: On the climate forcing of carbon monoxide, *J. Geophys. Res.-Atmos.*, 103, 13249–13260, doi:10.1029/98jd00822, 1998.

Deeter, M. N., Worden, H. M., Gille, J. C., Edwards, D. P., Mao, D., and Drummond, J. R.: MOPITT multispectral CO retrievals: origins and effects of geophysical radiance errors, *J. Geophys. Res.-Atmos.*, 116, D15303, doi:10.1029/2011jd015703, 2011.

## Implications of model bias in carbon monoxide for methane lifetime

S. A. Strode et al.

Title Page

Abstract

Introduction

Conclusions

References

Tables

Figures



Back

Close

Full Screen / Esc

Printer-friendly Version

Interactive Discussion



Deeter, M. N., Martinez-Alonso, S., Edwards, D. P., Emmons, L. K., Gille, J. C., Worden, H. M., Pittman, J. V., Daube, B. C., and Wofsy, S. C.: Validation of MOPITT Version 5 thermal-infrared, near-infrared, and multispectral carbon monoxide profile retrievals for 2000–2011, *J. Geophys. Res.-Atmos.*, 118, 6710–6725, doi:10.1002/jgrd.50272, 2013.

Derwent, R. G., Collins, W. J., Johnson, C. E., and Stevenson, D. S.: Transient behaviour of tropospheric ozone precursors in a global 3-D CTM and their indirect greenhouse effects, *Climatic Change*, 49, 463–487, doi:10.1023/a:1010648913655, 2001.

Duncan, B., Portman, D., Bey, I., and Spivakovsky, C.: Parameterization of OH for efficient computation in chemical tracer models, *J. Geophys. Res.-Atmos.*, 105, 12259–12262, doi:10.1029/1999jd901141, 2000.

Duncan, B. N. and Logan, J. A.: Model analysis of the factors regulating the trends and variability of carbon monoxide between 1988 and 1997, *Atmos. Chem. Phys.*, 8, 7389–7403, doi:10.5194/acp-8-7389-2008, 2008.

Duncan, B. N., Logan, J. A., Bey, I., Megretskaia, I. A., Yantosca, R. M., Novelli, P. C., Jones, N. B., and Rinsland, C. P.: Global budget of CO, 1988–1997: source estimates and validation with a global model, *J. Geophys. Res.-Atmos.*, 112, D22301, doi:10.1029/2007jd008459, 2007a.

Duncan, B. N., Strahan, S. E., Yoshida, Y., Steenrod, S. D., and Livesey, N.: Model study of the cross-tropopause transport of biomass burning pollution, *Atmos. Chem. Phys.*, 7, 3713–3736, doi:10.5194/acp-7-3713-2007, 2007b.

Edwards, D. P., Emmons, L. K., Hauglustaine, D. A., Chu, D. A., Gille, J. C., Kaufman, Y. J., Petron, G., Yurganov, L. N., Giglio, L., Deeter, M. N., Yudin, V., Ziskin, D. C., Warner, J., Lamarque, J. F., Francis, G. L., Ho, S. P., Mao, D., Chen, J., Grechko, E. I., and Drummond, J. R.: Observations of carbon monoxide and aerosols from the Terra satellite: Northern Hemisphere variability, *J. Geophys. Res.-Atmos.*, 109, D24202, doi:10.1029/2004jd004727, 2004.

Emmons, L. K., Deeter, M. N., Gille, J. C., Edwards, D. P., Attie, J. L., Warner, J., Ziskin, D., Francis, G., Khattatov, B., Yudin, V., Lamarque, J. F., Ho, S. P., Mao, D., Chen, J. S., Drummond, J., Novelli, P., Sachse, G., Coffey, M. T., Hannigan, J. W., Gerbig, C., Kawakami, S., Kondo, Y., Takegawa, N., Schlager, H., Baehr, J., and Ziereis, H.: Validation of Measurements of Pollution in the Troposphere (MOPITT) CO retrievals with aircraft in situ profiles, *J. Geophys. Res.-Atmos.*, 109, D03309, doi:10.1029/2003jd004101, 2004.

## Implications of model bias in carbon monoxide for methane lifetime

S. A. Strode et al.

Title Page

Abstract

Introduction

Conclusions

References

Tables

Figures



Back

Close

Full Screen / Esc

Printer-friendly Version

Interactive Discussion



Fortems-Cheiney, A., Chevallier, F., Pison, I., Bousquet, P., Szopa, S., Deeter, M. N., and Clerbaux, C.: Ten years of CO emissions as seen from Measurements of Pollution in the Troposphere (MOPITT), *J. Geophys. Res.-Atmos.*, 116, D05304, doi:10.1029/2010jd014416, 2011.

5 Fry, M. M., Naik, V., West, J. J., Schwarzkopf, M. D., Fiore, A. M., Collins, W. J., Dentener, F. J., Shindell, D. T., Atherton, C., Bergmann, D., Duncan, B. N., Hess, P., MacKenzie, I. A., Marmar, E., Schultz, M. G., Szopa, S., Wild, O., and Zeng, G.: The influence of ozone precursor emissions from four world regions on tropospheric composition and radiative climate forcing, *J. Geophys. Res.-Atmos.*, 117, D07306, doi:10.1029/2011jd017134, 2012.

10 Fry, M. M., Schwarzkopf, M. D., Adelman, Z., Naik, V., Collins, W. J., and West, J. J.: Net radiative forcing and air quality responses to regional CO emission reductions, *Atmos. Chem. Phys.*, 13, 5381–5399, doi:10.5194/acp-13-5381-2013, 2013.

Fuglestedt, J. S., Isaksen, I. S. A., and Wang, W. C.: Estimates of indirect global warming potentials for CH<sub>4</sub>, CO and NO<sub>x</sub>, *Climatic Change*, 34, 405–437, doi:10.1007/bf00139300, 15 1996.

Holloway, T., Levy, H., and Kasibhatla, P.: Global distribution of carbon monoxide, *J. Geophys. Res.-Atmos.*, 105, 12123–12147, doi:10.1029/1999jd901173, 2000.

10 Holmes, C. D., Prather, M. J., Søvde, O. A., and Myhre, G.: Future methane, hydroxyl, and their uncertainties: key climate and emission parameters for future predictions, *Atmos. Chem. Phys.*, 13, 285–302, doi:10.5194/acp-13-285-2013, 2013.

Hooghiemstra, P. B., Krol, M. C., Meirink, J. F., Bergamaschi, P., van der Werf, G. R., Novelli, P. C., Aben, I., and Röckmann, T.: Optimizing global CO emission estimates using a four-dimensional variational data assimilation system and surface network observations, *Atmos. Chem. Phys.*, 11, 4705–4723, doi:10.5194/acp-11-4705-2011, 2011.

25 IPCC: Climate Change: the IPCC Scientific Assessment, edited by: Houghton, J. T., Jenkins, G. J., and Ephraums, J. J., Cambridge University Press, 1990.

Johnson, C. E. and Derwent, R. G.: Relative radiative forcing consequences of global emissions of hydrocarbons, carbon monoxide and NO<sub>x</sub> from human activities estimated with a zonally-averaged two-dimensional model, *Climatic Change*, 34, 439–462, doi:10.1007/bf00139301, 30 1996.

Jones, D. B. A., Bowman, K. W., Logan, J. A., Heald, C. L., Liu, J., Luo, M., Worden, J., and Drummond, J.: The zonal structure of tropical O<sub>3</sub> and CO as observed by the Tropospheric

**Implications of model bias in carbon monoxide for methane lifetime**

S. A. Strode et al.

Title Page

Abstract

Introduction

Conclusions

References

Tables

Figures

◀

▶

◀

▶

Back

Close

Full Screen / Esc

Printer-friendly Version

Interactive Discussion



Emission Spectrometer in November 2004 – Part 1: Inverse modeling of CO emissions, Atmos. Chem. Phys., 9, 3547–3562, doi:10.5194/acp-9-3547-2009, 2009.

Kopacz, M., Jacob, D. J., Fisher, J. A., Logan, J. A., Zhang, L., Megretskaia, I. A., Yantosca, R. M., Singh, K., Henze, D. K., Burrows, J. P., Buchwitz, M., Khlystova, I., McMillan, W. W., Gille, J. C., Edwards, D. P., Eldering, A., Thouret, V., and Nedelec, P.: Global estimates of CO sources with high resolution by adjoint inversion of multiple satellite datasets (MOPITT, AIRS, SCIAMACHY, TES), Atmos. Chem. Phys., 10, 855–876, doi:10.5194/acp-10-855-2010, 2010.

Lamarque, J.-F., Shindell, D. T., Josse, B., Young, P. J., Cionni, I., Eyring, V., Bergmann, D., Cameron-Smith, P., Collins, W. J., Doherty, R., Dalsoren, S., Faluvegi, G., Folberth, G., Ghan, S. J., Horowitz, L. W., Lee, Y. H., MacKenzie, I. A., Nagashima, T., Naik, V., Plummer, D., Righi, M., Rumbold, S. T., Schulz, M., Skeie, R. B., Stevenson, D. S., Strode, S., Sudo, K., Szopa, S., Voulgarakis, A., and Zeng, G.: The Atmospheric Chemistry and Climate Model Intercomparison Project (ACCMIP): overview and description of models, simulations and climate diagnostics, Geosci. Model Dev., 6, 179–206, doi:10.5194/gmd-6-179-2013, 2013.

Mao, J., Fan, S., Jacob, D. J., and Travis, K. R.: Radical loss in the atmosphere from Cu-Fe redox coupling in aerosols, Atmos. Chem. Phys., 13, 509–519, doi:10.5194/acp-13-509-2013, 2013.

Miyazaki, K., Eskes, H. J., Sudo, K., Takigawa, M., van Weele, M., and Boersma, K. F.: Simultaneous assimilation of satellite NO<sub>2</sub>, O<sub>3</sub>, CO, and HNO<sub>3</sub> data for the analysis of tropospheric chemical composition and emissions, Atmos. Chem. Phys., 12, 9545–9579, doi:10.5194/acp-12-9545-2012, 2012.

Molod, A., Takacs, L., Suarez, M., Bacmeister, J., Song, I.-S., and Eichmann, A.: The GEOS-5 atmospheric general circulation model: mean climate and development from MERRA to Fortuna, NASA, Goddard Space Flight Center, Greenbelt, MD, 2012.

Monks, S. A., Arnold, S. R., Emmons, L. K., Law, K. S., Turquety, S., Duncan, B. N., Fleming, J., Huijnen, V., Tilmes, S., Langner, J., Mao, J., Long, Y., Thomas, J. L., Steenrod, S. D., Raut, J. C., Wilson, C., Chipperfield, M. P., Diskin, G. S., Weinheimer, A., Schlager, H., and Ancellet, G.: Multi-model study of chemical and physical controls on transport of anthropogenic and biomass burning pollution to the Arctic, Atmos. Chem. Phys., 15, 3575–3603, doi:10.5194/acp-15-3575-2015, 2015.

**Implications of model bias in carbon monoxide for methane lifetime**

S. A. Strode et al.

Title Page

Abstract

Introduction

Conclusions

References

Tables

Figures



Back

Close

Full Screen / Esc

Printer-friendly Version

Interactive Discussion



Morgenstern, O., Giorgetta, M. A., Shibata, K., Eyring, V., Waugh, D. W., Shepherd, T. G., Akiyoshi, H., Austin, J., Baumgaertner, A. J. G., Bekki, S., Braesicke, P., Bruhl, C., Chipperfield, M. P., Cugnet, D., Dameris, M., Dhomse, S., Frith, S. M., Garny, H., Gettelman, A., Hardiman, S. C., Hegglin, M. I., Jockel, P., Kinnison, D. E., Lamarque, J. F., Mancini, E., Manzini, E., Marchand, M., Michou, M., Nakamura, T., Nielsen, J. E., Olivie, D., Pitari, G., Plummer, D. A., Rozanov, E., Scinocca, J. F., Smale, D., Teysedre, H., Toohey, M., Tian, W., and Yamashita, Y.: Review of the formulation of present-generation stratospheric chemistry-climate models and associated external forcings, *J. Geophys. Res.-Atmos.*, 115, D00M02, doi:10.1029/2009jd013728, 2010.

Müller, J.-F. and Stavrakou, T.: Inversion of CO and NO<sub>x</sub> emissions using the adjoint of the IMAGES model, *Atmos. Chem. Phys.*, 5, 1157–1186, doi:10.5194/acp-5-1157-2005, 2005.

Murray, L. T., Logan, J. A., and Jacob, D. J.: Interannual variability in tropical tropospheric ozone and OH: the role of lightning, *J. Geophys. Res.-Atmos.*, 118, 11468–11480, doi:10.1002/jgrd.50857, 2013.

Murray, L. T., Mickley, L. J., Kaplan, J. O., Sofen, E. D., Pfeiffer, M., and Alexander, B.: Factors controlling variability in the oxidative capacity of the troposphere since the Last Glacial Maximum, *Atmos. Chem. Phys.*, 14, 3589–3622, doi:10.5194/acp-14-3589-2014, 2014.

Naik, V., Mauzerall, D., Horowitz, L., Schwarzkopf, M. D., Ramaswamy, V., and Oppenheimer, M.: Net radiative forcing due to changes in regional emissions of tropospheric ozone precursors, *J. Geophys. Res.-Atmos.*, 110, D24306, doi:10.1029/2005jd005908, 2005.

Naik, V., Voulgarakis, A., Fiore, A. M., Horowitz, L. W., Lamarque, J.-F., Lin, M., Prather, M. J., Young, P. J., Bergmann, D., Cameron-Smith, P. J., Cionni, I., Collins, W. J., Dalsøren, S. B., Doherty, R., Eyring, V., Faluvegi, G., Folberth, G. A., Josse, B., Lee, Y. H., MacKenzie, I. A., Nagashima, T., van Noije, T. P. C., Plummer, D. A., Righi, M., Rumbold, S. T., Skeie, R., Shindell, D. T., Stevenson, D. S., Strode, S., Sudo, K., Szopa, S., and Zeng, G.: Preindustrial to present-day changes in tropospheric hydroxyl radical and methane lifetime from the Atmospheric Chemistry and Climate Model Intercomparison Project (ACCMIP), *Atmos. Chem. Phys.*, 13, 5277–5298, doi:10.5194/acp-13-5277-2013, 2013.

Novelli, P. C. and Masarie, K. A.: Atmospheric Carbon Monoxide Dry Air Mole Fractions from the NOAA ESRL Carbon Cycle Cooperative Global Air Sampling Network, 1988–2013, Version: 2014-07-02, available at: ftp://aftp.cmdl.noaa.gov/data/trace\_gases/co/flask/surface/ (last access: June 2013), 2014.

**Implications of model bias in carbon monoxide for methane lifetime**

S. A. Strode et al.

Title Page

Abstract

Introduction

Conclusions

References

Tables

Figures



Back

Close

Full Screen / Esc

Printer-friendly Version

Interactive Discussion



- Patra, P. K., Krol, M. C., Montzka, S. A., Arnold, T., Atlas, E. L., Lintner, B. R., Stephens, B. B., Xiang, B., Elkins, J. W., Fraser, P. J., Ghosh, A., Hints, E. J., Hurst, D. F., Ishijima, K., Krummel, P. B., Miller, B. R., Miyazaki, K., Moore, F. L., Muhle, J., O'Doherty, S., Prinn, R. G., Steele, L. P., Takigawa, M., Wang, H. J., Weiss, R. F., Wofsy, S. C., and Young, D.: Observational evidence for interhemispheric hydroxyl-radical parity, *Nature*, 513, 219–223, doi:10.1038/nature13721, 2014.
- Petron, G., Granier, C., Khattatov, B., Yudin, V., Lamarque, J. F., Emmons, L., Gille, J., and Edwards, D. P.: Monthly CO surface sources inventory based on the 2000–2001 MOPITT satellite data, *Geophys. Res. Lett.*, 31, L21107, doi:10.1029/2004gl020560, 2004.
- Pison, I., Bousquet, P., Chevallier, F., Szopa, S., and Hauglustaine, D.: Multi-species inversion of CH<sub>4</sub>, CO and H<sub>2</sub> emissions from surface measurements, *Atmos. Chem. Phys.*, 9, 5281–5297, doi:10.5194/acp-9-5281-2009, 2009.
- Prather, M. J.: Time scales in atmospheric chemistry: theory, GWPs for CH<sub>4</sub> and CO, and runaway growth, *Geophys. Res. Lett.*, 23, 2597–2600, 1996.
- Prather, M. J., Holmes, C. D., and Hsu, J.: Reactive greenhouse gas scenarios: systematic exploration of uncertainties and the role of atmospheric chemistry, *Geophys. Res. Lett.*, 39, L09803, doi:10.1029/2012gl051440, 2012.
- Prinn, R. G., Huang, J., Weiss, R. F., Cunnold, D. M., Fraser, P. J., Simmonds, P. G., McCulloch, A., Harth, C., Reimann, S., Salameh, P., O'Doherty, S., Wang, R. H. J., Porter, L. W., Miller, B. R., and Krummel, P. B.: Evidence for variability of atmospheric hydroxyl radicals over the past quarter century, *Geophys. Res. Lett.*, 32, L07809, doi:10.1029/2004gl022228, 2005.
- Rienecker, M. M., Suarez, M. J., Gelaro, R., Todling, R., Bacmeister, J., Liu, E., Bosilovich, M. G., Schubert, S. D., Takacs, L., Kim, G.-K., Bloom, S., Chen, J., Collins, D., Conaty, A., da Silva, A., Gu, W., Joiner, J., Koster, R. D., Lucchesi, R., Molod, A., Owens, T., Pawson, S., Pegion, P., Redder, C. R., Reichle, R., Robertson, F. R., Ruddick, A. G., Sienkiewicz, M., and Woollen, J.: MERRA: NASA's Modern-Era Retrospective Analysis for Research and Applications, *J. Climate*, 24, 3624–3648, doi:10.1175/JCLI-D-11-00015.1, 2011.
- Rohrer, F. and Berresheim, H.: Strong correlation between levels of tropospheric hydroxyl radicals and solar ultraviolet radiation, *Nature*, 442, 184–187, 2006.
- Shindell, D. T., Faluvegi, G., Stevenson, D. S., Krol, M. C., Emmons, L. K., Lamarque, J. F., Petron, G., Dentener, F. J., Ellingsen, K., Schultz, M. G., Wild, O., Amann, M., Atherton, C. S.,

**Implications of model bias in carbon monoxide for methane lifetime**

S. A. Strode et al.

[Title Page](#)[Abstract](#)[Introduction](#)[Conclusions](#)[References](#)[Tables](#)[Figures](#)[Back](#)[Close](#)[Full Screen / Esc](#)[Printer-friendly Version](#)[Interactive Discussion](#)

Bergmann, D. J., Bey, I., Butler, T., Cofala, J., Collins, W. J., Derwent, R. G., Doherty, R. M., Drevet, J., Eskes, H. J., Fiore, A. M., Gauss, M., Hauglustaine, D. A., Horowitz, L. W., Isak-  
sen, I. S. A., Lawrence, M. G., Montanaro, V., Muller, J. F., Pitari, G., Prather, M. J., Pyle, J. A.,  
Rast, S., Rodriguez, J. M., Sanderson, M. G., Savage, N. H., Strahan, S. E., Sudo, K.,  
5 Szopa, S., Unger, N., van Noije, T. P. C., and Zeng, G.: Multimodel simulations of carbon  
monoxide: comparison with observations and projected near-future changes, *J. Geophys.*  
*Res.-Atmos.*, 111, D19306, doi:10.1029/2006jd007100, 2006.

Shindell, D. T., Faluvegi, G., Koch, D. M., Schmidt, G. A., Unger, N., and Bauer, S. E.:  
Improved attribution of climate forcing to emissions, *Science*, 326, 716–718,  
10 doi:10.1126/science.1174760, 2009.

Spivakovsky, C. M., Logan, J. A., Montzka, S. A., Balkanski, Y. J., Foreman-Fowler, M.,  
Jones, D. B. A., Horowitz, L. W., Fusco, A. C., Brenninkmeijer, C. A. M., Prather, M. J.,  
Wofsy, S. C., and McElroy, M. B.: Three-dimensional climatological distribution of tro-  
pospheric OH: update and evaluation, *J. Geophys. Res.-Atmos.*, 105, 8931–8980,  
15 doi:10.1029/1999jd901006, 2000.

Strahan, S. E., Duncan, B. N., and Hoor, P.: Observationally derived transport diagnostics for  
the lowermost stratosphere and their application to the GMI chemistry and transport model,  
*Atmos. Chem. Phys.*, 7, 2435–2445, doi:10.5194/acp-7-2435-2007, 2007.

Strode, S. A. and Pawson, S.: Detection of carbon monoxide trends in the presence of interan-  
20 nual variability, *J. Geophys. Res.-Atmos.*, 118, 12257–12273, doi:10.1002/2013JD020258,  
2013.

Voulgarakis, A., Naik, V., Lamarque, J.-F., Shindell, D. T., Young, P. J., Prather, M. J., Wild, O.,  
Field, R. D., Bergmann, D., Cameron-Smith, P., Cionni, I., Collins, W. J., Dalsøren, S. B.,  
Doherty, R. M., Eyring, V., Faluvegi, G., Folberth, G. A., Horowitz, L. W., Josse, B., MacKen-  
zie, I. A., Nagashima, T., Plummer, D. A., Righi, M., Rumbold, S. T., Stevenson, D. S.,  
25 Strode, S. A., Sudo, K., Szopa, S., and Zeng, G.: Analysis of present day and future OH  
and methane lifetime in the ACCMIP simulations, *Atmos. Chem. Phys.*, 13, 2563–2587,  
doi:10.5194/acp-13-2563-2013, 2013.

Wargan, K., Pawson, S., Olsen, M. A., Witte, J. C., Douglass, A. R., Ziemke, J. R., Stra-  
han, S. E., and Nielsen, J. E.: The global structure of upper troposphere-lower stratosphere  
30 ozone in GEOS-5: a multiyear assimilation of EOS Aura data, *J. Geophys. Res.-Atmos.*, 120,  
JD022493, doi:10.1002/2014JD022493, 2015.

Young, P. J., Archibald, A. T., Bowman, K. W., Lamarque, J.-F., Naik, V., Stevenson, D. S., Tilmes, S., Voulgarakis, A., Wild, O., Bergmann, D., Cameron-Smith, P., Cionni, I., Collins, W. J., Dalsøren, S. B., Doherty, R. M., Eyring, V., Faluvegi, G., Horowitz, L. W., Josse, B., Lee, Y. H., MacKenzie, I. A., Nagashima, T., Plummer, D. A., Righi, M., Rumbold, S. T., Skeie, R. B., Shindell, D. T., Strode, S. A., Sudo, K., Szopa, S., and Zeng, G.: Pre-industrial to end 21st century projections of tropospheric ozone from the Atmospheric Chemistry and Climate Model Intercomparison Project (ACCMIP), *Atmos. Chem. Phys.*, 13, 2063–2090, doi:10.5194/acp-13-2063-2013, 2013.

Ziemke, J. R., Chandra, S., Labow, G. J., Bhartia, P. K., Froidevaux, L., and Witte, J. C.: A global climatology of tropospheric and stratospheric ozone derived from Aura OMI and MLS measurements, *Atmos. Chem. Phys.*, 11, 9237–9251, doi:10.5194/acp-11-9237-2011, 2011.

Ziemke, J. R., Olsen, M. A., Witte, J. C., Douglass, A. R., Strahan, S. E., Wargan, K., Liu, X., Schoeberl, M. R., Yang, K., Kaplan, T. B., Pawson, S., Duncan, B. N., Newman, P. A., Bhartia, P. K., and Heney, M. K.: Assessment and applications of NASA ozone data products derived from Aura OMI/MLS satellite measurements in context of the GMI chemical transport model, *J. Geophys. Res.-Atmos.*, 119, 5671–5699, doi:10.1002/2013jd020914, 2014.

ACPD

15, 20305–20348, 2015

## Implications of model bias in carbon monoxide for methane lifetime

S. A. Strode et al.

Title Page

Abstract

Introduction

Conclusions

References

Tables

Figures

◀

▶

◀

▶

Back

Close

Full Screen / Esc

Printer-friendly Version

Interactive Discussion



## Implications of model bias in carbon monoxide for methane lifetime

S. A. Strode et al.

Title Page

Abstract

Introduction

Conclusions

References

Tables

Figures



Back

Close

Full Screen / Esc

Printer-friendly Version

Interactive Discussion



**Table 1.** Description of reference and sensitivity simulations used in this study with each chemistry option.

Simulation	Description	Key Result
GMI chemistry simulations		
RefGMI*	ACCMIP timeslice simulation for 2000	CO biased low at high latitudes
GMI-HiEmis	increased CO emissions compared to RefGMI	Regional CO biases compared to MOPITT
CO-only simulations		
RefCOonly*	Tagged-CO version of RefGMI	Similar CO biases to RefGMI
COonlyLowNHOH	NH OH uniformly decreased by 20 %	Improves agreement with GMD CO observations
COonlySD	meteorology constrained by MERRA (specified dynamics)	Improves agreement with GMD CO observations in summer
CO-OH simulations		
RefCO-OH*	Parameterized OH version of RefGMI	Lower OH than RefGMI
CO-OHSensTCO	tropospheric ozone column adjusted to match OMI/MLS TCO	Small increase in CH <sub>4</sub> lifetime
CO-OHSensStO3	stratospheric O <sub>3</sub> adjusted to match assimilated O <sub>3</sub>	Small increase in CH <sub>4</sub> lifetime
CO-OHSensQ	tropospheric water vapor adjusted based on MERRA	Increase in CH <sub>4</sub> lifetime
CO-OHSensNOx	30 % decrease in NH NO <sub>x</sub> concentrations	Small increase in CH <sub>4</sub> lifetime; OH asymmetry reduced but not eliminated
CO-OHSensAll	tropospheric and stratospheric O <sub>3</sub> , water vapor, and NH NO <sub>x</sub> all adjusted	15 % increase in CH <sub>4</sub> lifetime; OH asymmetry reduced but not eliminated

\* Reference simulation.

## Implications of model bias in carbon monoxide for methane lifetime

S. A. Strode et al.

Title Page

Abstract

Introduction

Conclusions

References

Tables

Figures

◀

▶

◀

▶

Back

Close

Full Screen / Esc

Printer-friendly Version

Interactive Discussion



**Table 2.** Tropospheric OH concentrations and lifetimes against oxidation by tropospheric OH.

	RefGMI	GMI-HiEmis	RefCO-OH
Global Mean OH ( $10^6 \text{ molec cm}^{-3}$ )	1.14	1.11	1.051
SH OH ( $10^6 \text{ molec cm}^{-3}$ )	1.03	1.02	0.943
NH OH ( $10^6 \text{ molec cm}^{-3}$ )	1.22	1.18	1.15
NH/SH OH	1.19	1.16	1.22
CH <sub>4</sub> lifetime (years)	9.65	9.89	10.5
CH <sub>3</sub> CCl <sub>3</sub> lifetime (years)	5.91	6.06	6.39

## Implications of model bias in carbon monoxide for methane lifetime

S. A. Strode et al.

Title Page

Abstract

Introduction

Conclusions

References

Tables

Figures



Back

Close

Full Screen / Esc

Printer-friendly Version

Interactive Discussion



**Table 3.** CO emission adjustment for the high emission simulation compared to the standard simulation.

Emission Increase (%)	Months			
	Jan–Feb	Mar–May	Jun–Aug	Sep–Dec
Asian and European anthropogenic	17.4	45.0	63.2	0.00
Russian BB	17.4	45.0	63.2	0.00
Tropical BB	26.4	60.6	28.2	0.00

## Implications of model bias in carbon monoxide for methane lifetime

S. A. Strode et al.

Title Page

Abstract

Introduction

Conclusions

References

Tables

Figures

⏪

⏩

◀

▶

Back

Close

Full Screen / Esc

Printer-friendly Version

Interactive Discussion



**Table 4.** NH<sub>2</sub>/SH OH ratio and percent changes in tropospheric OH concentrations and lifetimes against tropospheric OH for the CO-OH sensitivity studies compared to the RefCO-OH simulation.

	SensTCO	SensStO3	SensQ	SensNOx	SensAll
NH <sub>2</sub> /SH OH	1.19	1.23	1.22	1.15	1.14
	% change vs. RefCO-OH				
Global Mean OH	-2.1	-2.1	-6.2	-3.1	-13
SH OH	-1	-2.9	-6.3	-0.3	-10
NH OH	-3.1	-1.5	-6.1	-5.7	-16
CH <sub>4</sub> lifetime	2.5	2.4	5.7	3.5	15
CH <sub>3</sub> CCl <sub>3</sub> lifetime	2.4	2.3	5.9	3.5	15

## Implications of model bias in carbon monoxide for methane lifetime

S. A. Strode et al.

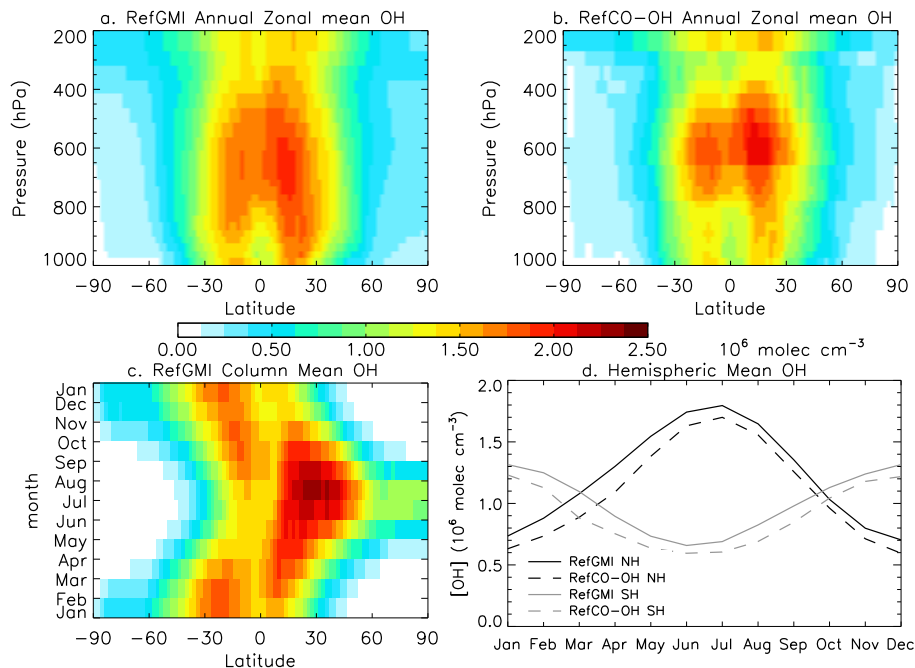


**Figure 1.** Simulated annual zonal mean OH concentration for the RefGMI (a) and RefCO-OH simulations (b) averaged over 1999–2009. (c) The annual cycle of the pressure-weighted column mean OH by latitude from the RefGMI simulation. The column is averaged between the surface and 200 hPa. (d) The annual cycle of hemispheric mean OH from the RefGMI (solid lines) and RefCO-OH (dashed lines) simulations for the Northern Hemisphere (black lines) and Southern Hemisphere (gray lines).

[Title Page](#)
[Abstract](#)
[Introduction](#)
[Conclusions](#)
[References](#)
[Tables](#)
[Figures](#)
[Back](#)
[Close](#)
[Full Screen / Esc](#)
[Printer-friendly Version](#)
[Interactive Discussion](#)

## Implications of model bias in carbon monoxide for methane lifetime

S. A. Strode et al.

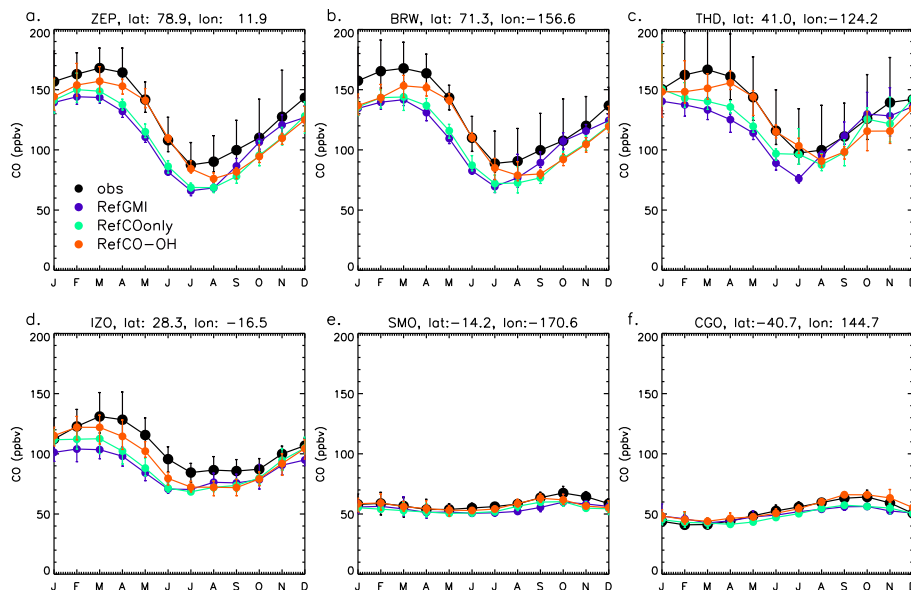


**Figure 2.** Monthly mean GMD observations (black) and results from the RefGMI (purple), RefCOonly (green), and RefCO-OH (orange) simulations. Circles and error bars represent the mean and min-max range, respectively, for 1999–2009. The GMD sites are as follows: **(a)** Ny-Alesund, Svalbard (ZEP, 78.9° N, 11.9° E), **(b)** Barrow, Alaska (BRW, 71.3° N, 156.6° W), **(c)** Trinidad Head, California (THD, 41.0° N, 124.2° W), **(d)** Izana, Tenerife, Canary Islands (IZO, 28.3° N, 16.5° W), Tutuila, American Samoa (SMO, 14.2° S, 170.6° W), and **(e)** Cape Grim, Tasmania (CGO, 40.7° S, 144.7° E).

[Title Page](#)
[Abstract](#)
[Introduction](#)
[Conclusions](#)
[References](#)
[Tables](#)
[Figures](#)
[Back](#)
[Close](#)
[Full Screen / Esc](#)
[Printer-friendly Version](#)
[Interactive Discussion](#)

## Implications of model bias in carbon monoxide for methane lifetime

S. A. Strode et al.

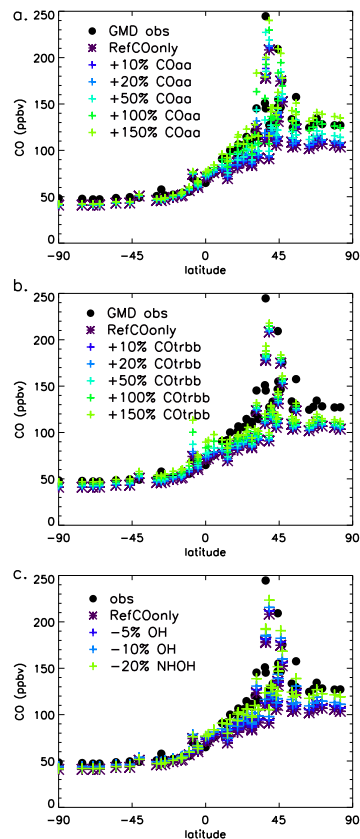


**Figure 3.** Latitudinal distribution of CO observations from the GMD network (black circles) and simulated CO from the RefCOonly simulation (purple stars) averaged over March–August. Blue-green + signs indicate the effect of **(a)** increasing the Asian anthropogenic CO tracer, **(b)** increasing the tropical biomass burning CO tracer, and **(c)** decreasing OH globally by 5 or 10 %, or decreasing NH OH by 20 %.

[Title Page](#)
[Abstract](#)
[Introduction](#)
[Conclusions](#)
[References](#)
[Tables](#)
[Figures](#)
[Back](#)
[Close](#)
[Full Screen / Esc](#)
[Printer-friendly Version](#)
[Interactive Discussion](#)

## Implications of model bias in carbon monoxide for methane lifetime

S. A. Strode et al.

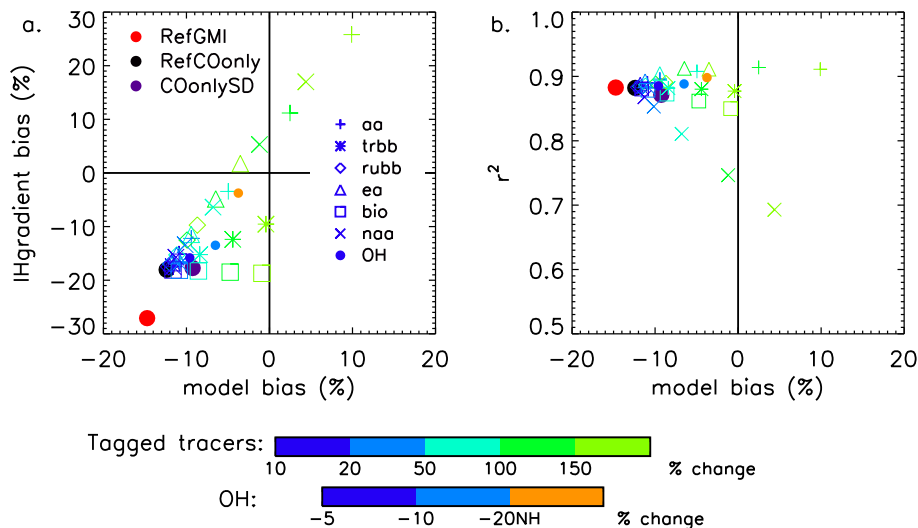


**Figure 4.** The impact of increasing the tagged CO tracers for Asian anthropogenic (+), tropical biomass burning (star), Russian biomass burning (diamonds), European anthropogenic (triangles), biogenic (squares), and North American anthropogenic (×) sources on **(a)** bias in the inter-hemispheric gradient vs. global mean bias and **(b)** correlation vs. global mean bias compared to GMD observations from March-May. Large circles represent the RefGMI (red), RefCOonly (black), and COonlySD (purple) simulations. Small circles show the impact of changing global or NH OH in the RefCOonly simulation.

[Title Page](#)
[Abstract](#)
[Introduction](#)
[Conclusions](#)
[References](#)
[Tables](#)
[Figures](#)
[Back](#)
[Close](#)
[Full Screen / Esc](#)
[Printer-friendly Version](#)
[Interactive Discussion](#)

Implications of model bias in carbon monoxide for methane lifetime

S. A. Strode et al.

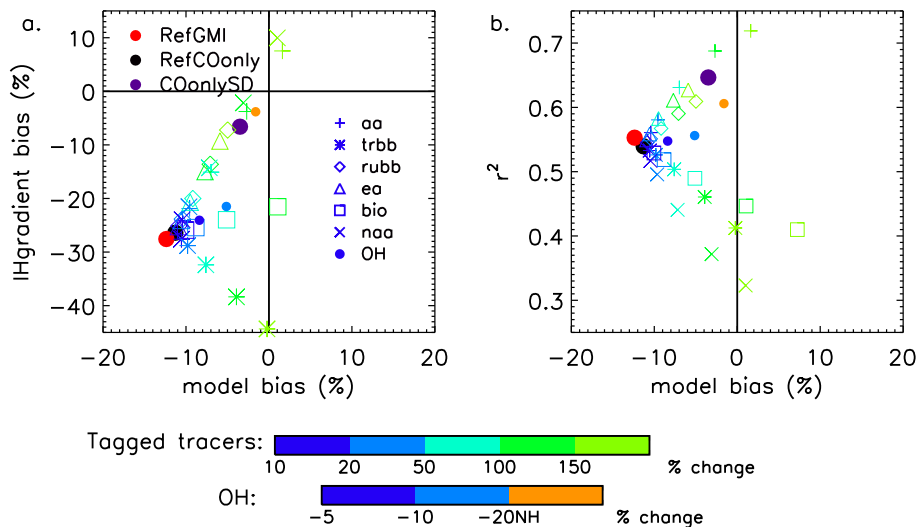


Figure 5. As in Fig. 4, but for June through August.

Title Page

Abstract

Introduction

Conclusions

References

Tables

Figures

◀

▶

◀

▶

Back

Close

Full Screen / Esc

Printer-friendly Version

Interactive Discussion



## Implications of model bias in carbon monoxide for methane lifetime

S. A. Strode et al.

Title Page

Abstract

Introduction

Conclusions

References

Tables

Figures



Back

Close

Full Screen / Esc

Printer-friendly Version

Interactive Discussion

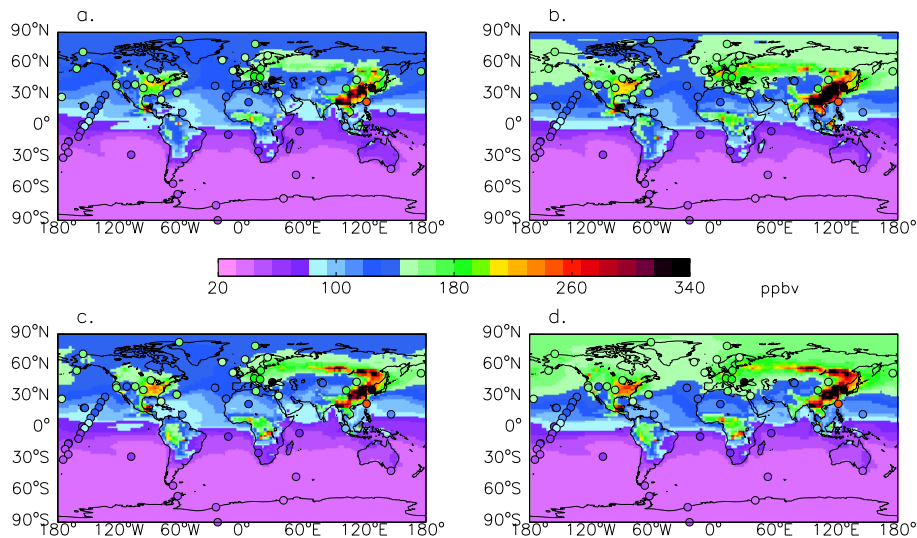


**Figure 6.** CO for April 2007 from the GMD observations (circles) overlotted on the surface CO from (a) RefGMI, (b) GMI-HiEmis, (c) RefCOonly, and (d) COonlyLowNHOH simulations.

## Implications of model bias in carbon monoxide for methane lifetime

S. A. Strode et al.

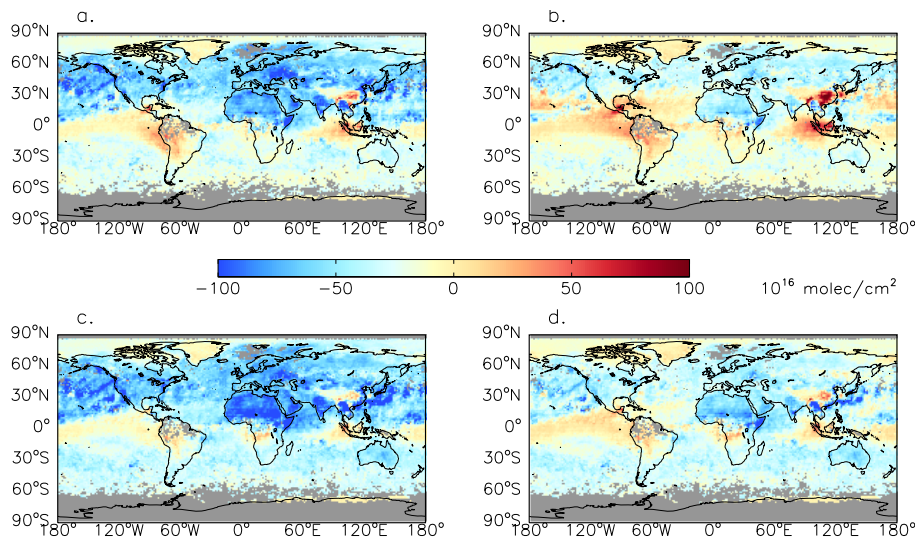


**Figure 7.** April 2007 difference between the simulated CO columns and MOPITT for the (a) RefGMI, (b) GMI-HiEmis, (c) RefCOonly, and (d) COonlyLowNHOH simulations. The simulated CO is convolved with the MOPITT averaging kernels and a priori.

[Title Page](#)[Abstract](#)[Introduction](#)[Conclusions](#)[References](#)[Tables](#)[Figures](#)[◀](#)[▶](#)[◀](#)[▶](#)[Back](#)[Close](#)[Full Screen / Esc](#)[Printer-friendly Version](#)[Interactive Discussion](#)



**Implications of model bias in carbon monoxide for methane lifetime**

S. A. Strode et al.

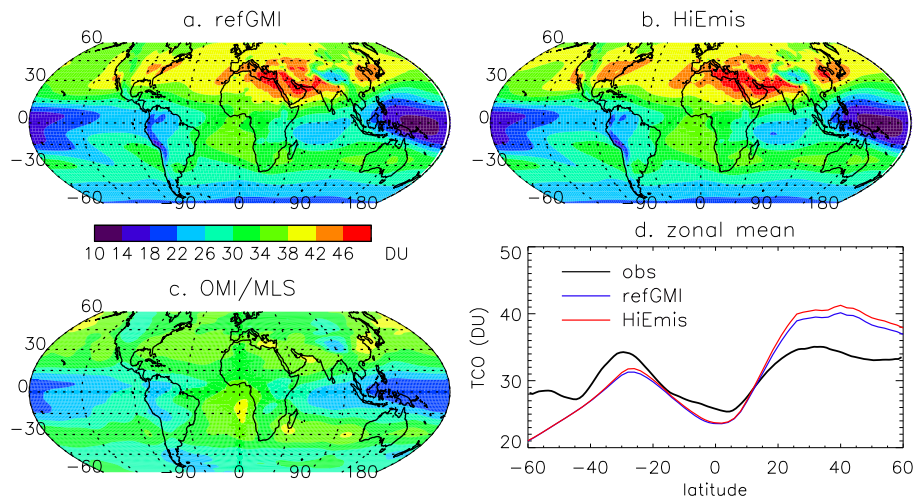


**Figure 9.** Annual mean tropospheric column ozone (TCO) from the RefGMI (a) and GMI-HiEmis (b) simulations compared to the OMI/MLS TCO product (c) of Ziemke et al. (2011). (d) compares the zonal mean simulated and OMI/MLS values. The simulated values are averaged over the years of the timeslice (1999–2009).

[Title Page](#)[Abstract](#)[Introduction](#)[Conclusions](#)[References](#)[Tables](#)[Figures](#)[◀](#)[▶](#)[◀](#)[▶](#)[Back](#)[Close](#)[Full Screen / Esc](#)[Printer-friendly Version](#)[Interactive Discussion](#)

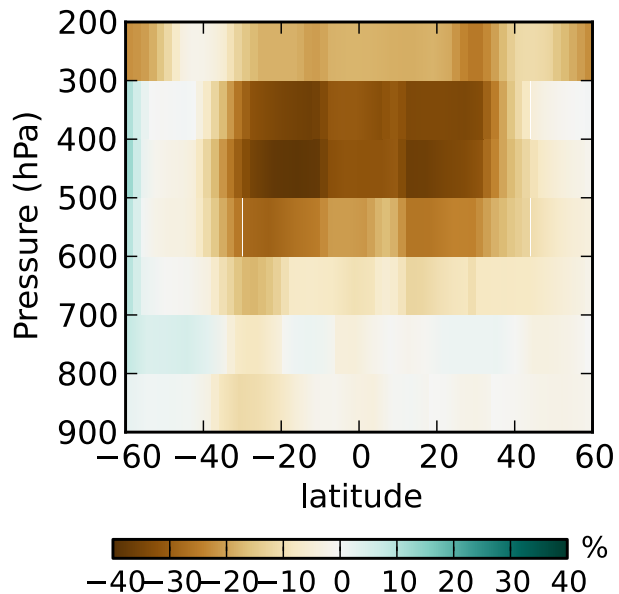


**Figure 10.** Annual mean percent change in specific humidity imposed in the CO-OHSensQ experiment between 900 and 200 hPa, 60° S–60° N.

**Implications of model bias in carbon monoxide for methane lifetime**

S. A. Strode et al.

[Title Page](#)

[Abstract](#) | [Introduction](#)

[Conclusions](#) | [References](#)

[Tables](#) | [Figures](#)

[◀](#) | [▶](#)

[◀](#) | [▶](#)

[Back](#) | [Close](#)

[Full Screen / Esc](#)

[Printer-friendly Version](#)

[Interactive Discussion](#)



**Implications of model bias in carbon monoxide for methane lifetime**

S. A. Strode et al.

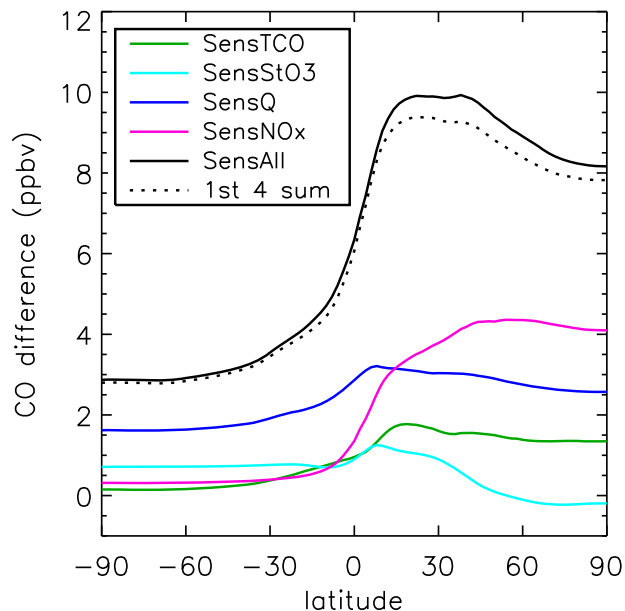


**Figure 11.** Zonal mean surface CO difference compared to RefCO-OH for the CO-OHSensTCO (green), CO-OHSensStO3 (cyan), CO-OHSensQ (blue), CO-OHSensNOx (pink), and CO-OHSensAll (solid black) simulations averaged over March through August of 2005 to 2009. The sum of the differences for the CO-OHSensTCO, CO-OHSensStO3, CO-OHSensQ, and CO-OHSensNOx compared to RefCO-OH is shown in the black dotted line.

[Title Page](#)[Abstract](#)[Introduction](#)[Conclusions](#)[References](#)[Tables](#)[Figures](#)[◀](#)[▶](#)[◀](#)[▶](#)[Back](#)[Close](#)[Full Screen / Esc](#)[Printer-friendly Version](#)[Interactive Discussion](#)